INFORMATIVE WAVELENGTHS FOR TRACE ATMOSPHERIC GAS SOUNDING WITH AN OPO-LIDAR IN THE 3–4 μm SPECTRAL REGION

Romanovskii O.A.[*a,b], Kharchenko O.V.[a], Sadovnikov S.A.[a], Yakovlev S.V.[a,b]
[a] V.E. Zuev Institute of Atmospheric Optics, Siberian Branch, Russian Academy of Sciences, 1 Academician V.E. Zuev Square, Tomsk 634021 Russia;
[b] National Research Tomsk State University, 36 Lenin Ave., Tomsk, 634050 Russia

ABSTRACT

In this work, a search for information-bearing mid-IR wavelengths for HCl and HBr sounding with a differential absorption lidar based on an optical parametric oscillator has been carried out. Lidar echo signals have been calculated at the wavelengths chosen during sounding of gas components along vertical paths 0–5 km long.

Keywords: lidar, informative wavelengths, echo-signal, atmosphere, OPO.

1. INTRODUCTION

Remote monitoring of concentrations of trace atmospheric gases (TAGs), including many noxious admixtures, remains an urgent problem. The IR region, especially the 2.5–14 μm range, is very promising for atmospheric sounding, since this range includes strong absorption lines of almost all atmospheric gases. In addition, the IR range includes six transparency windows. To cover the near- and mid-IR range, radiation of optical parametric oscillators (OPO) on the basis of nonlinear crystals is often used [1–3]. In this work, we consider a laser system (designed at SOLAR laser system company), which is a part of a differential absorption lidar designed; it provides tunable generation of nanosecond radiation pulses in the 3–4 μm spectral range. Possibility of HCl and HBr sounding along tropospheric paths in this spectral range is estimated on the basis of specifications of the laser. Results of search for informative wavelengths and calculation of lidar echo signals during differential-absorption sounding of the above gases are presented.

2. LASER PARAMETERS

The laser system includes:
- LQ529B Nd:YAG pulsed laser;
- radiation converter with the wavelength tuning range 3–4 μm;
- step-motor (SM) wavelength control;
- SM controller;
- S100 spectrometer;
- base for the laser and the radiation converter with a system for pumping radiation guiding to the converter.

Specifications of the pumping laser and radiation converter are given in Tables 1 and 2.

Table 1. Specifications of LQ529B pumping laser

Pulse frequency	10 Hz
Output energy: at 1064 nm	350 mJ
Pulse length at 1064 nm, FWHM	10...13 ns
Beam diameter at 1064 nm	≤ 6 mm
Divergence angle at 1064 nm	~ 1.5 mrad
Stability of pulse energy at 1064 nm, better than	± 2.5 %

* e-mail: roa@iao.ru; Phone 7 3822 490462; fax 7 3822 492086

21st International Symposium on Atmospheric and Ocean Optics: Atmospheric Physics, edited by G. G. Matvienko, O. A. Romanovskii, Proc. of SPIE Vol. 9680, 96803W
 · doi: 10.1117/12.2205678

Table 2. Specifications of radiation converter

Wavelength tuning range	3…4 μm
Radiation line width	< 5 cm^{-1}
Pulse energy, in the tuning curve peak	> 5
Pulse frequency	10 Hz
Radiation divergence angle	</= 2 mrad
Wavelength tuning control	by 3 SMs

The optical scheme of the radiation converter corresponds to an OPO/OPA scheme.

The converter includes KTP-crystal based OPO pumped with 2nd harmonic 532-nm radiation and KTA-crystal based optical parametric amplifier (OPA) pumped with 1024-nm radiation.

The OPO is intended for generation of low-power radiation with a pumping tunable wavelength in the 0.785–0.840 μm (signal wave λ_s) and 1.45–1.65 μm (idler wave λ_i) regions. The wavelengths are related as $1/\lambda_1 = 1/\lambda_3 - 1/\lambda_2$, where $\lambda_3 = 1.0642$ μm and $\lambda_2 = 1.45–1.65$ μm.

OPA is intended for generation and amplification of radiation with a tunable wavelength in the 3–4 μm region (the difference frequency λ_1). The wavelengths are related as $1/\lambda_1 = 1/\lambda_3 - 1/\lambda_2$, where $\lambda_3 = 1.0642$ μm, $\lambda_2 = 1.45 – 1.65$ μm.

The output radiation wavelength is controlled by a S100 built-in spectrometer. Using the spectrometer, the lasing wavelength of the signal wave λ_s, in μm, is determined. The wavelength of the difference frequency λ_1 in the 3–4 μm region is calculated by the equation $\lambda_1 = 1.0642\lambda_s/(1.0642 - \lambda_s)$. The converter design provides:

- possibility of mounting a SM-controlled selecting element (diffraction grating) in the oscillator cavity for narrowing the lasing line to 0.5 cm^{-1};
- possibility of mounting a single-frequency pumping laser for narrowing the lasing line to 0.1 cm^{-1};
- possibility of additional mounting of SLM injection laser diode for producing generation with the line width lower than 0.1 cm^{-1}.

3. SEARCH RESULTS OF INFORMATIVE WAVELENGTH FOR TAG SOUNDING

The technique [4] was tested to estimate capabilities of sounding TAGs with the use of a laser with OPO on the basis of nonlinear KTA crystal.

To analyze a possibility of using the OPO-laser radiation for remote laser atmospheric gas analysis, a spectrum of air transmittance was calculated. Hydrogen chloride and hydrogen bromide were taken for the analysis, since their fundamental rotational-vibrational absorption bands fall in the spectral range of radiation of the laser source considered in this work. The bands are of a quite simple and, hence, well studied structure. The total intensity of the HCl and HBr absorption bands is 4.5 10^{-18} and 7.2 10^{-19} cm/mol., respectively. The centers of individual absorption bands of these gases are equally spaced apart to about 15 cm^{-1} and have intensities of 4.5 10^{-19} and 6.5 10^{-20} cm/mol. for HCl and HBr, respectively.

The transmission spectra were line-by-line calculated with the use of data on spectral parameters of absorption lines of main atmospheric gases for a surface sounding path 1 km long and a standard atmospheric model (summer, midlatitude). During the calculations, the frequency step was 0.1 cm^{-1} for the radiation line width >1 cm^{-1} and <5 cm^{-1}. The calculations were carried out under the assumption that the concentration of a gas sounded is 1 ppm. The calculation results are shown in Figs. 1–4 and in Tables 3 and 4. The tables present pairs of wavelengths suitable for HCl and HBr sounding by the differential absorption method, as well as the transmission coefficients T_{TAG} along a surface path 1 km long when only the gas under study absorbs and the transmission coefficients of interfering gases typical for midlatitude summer (15600 ppm for H_2O, 338 ppm for CO_2, 30 ppb for ozone, 1.7 ppm for CH_4, 0.3 ppm for N_2O, 2.5 ppb for H_2CO, and 3.7 ppb for NO_2).

The calculations show that the radiation with a line width of about 1 cm^{-1} is preferable for HBr sounding, and the line width can vary in the 1–5 cm^{-1} limits in the case of HCl sounding. The laser system design provides for a possibility of mounting a diffraction grating in the cavity to narrow the lasing line to 0.5–1 cm^{-1}.

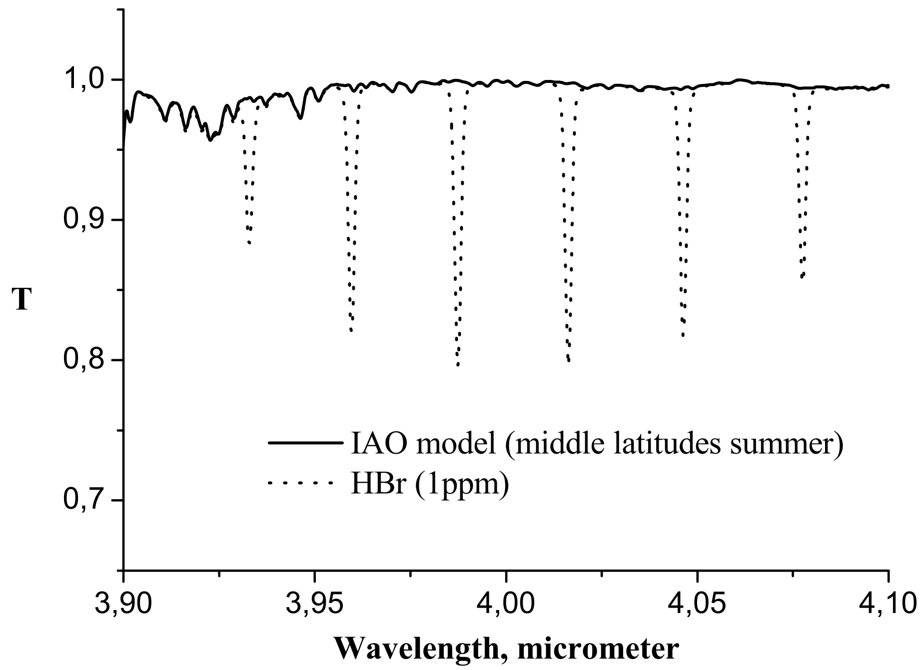

Figure 1. Air transmission spectrum for a path 1 km long (HBr; lasing line width 1 cm^{-1})

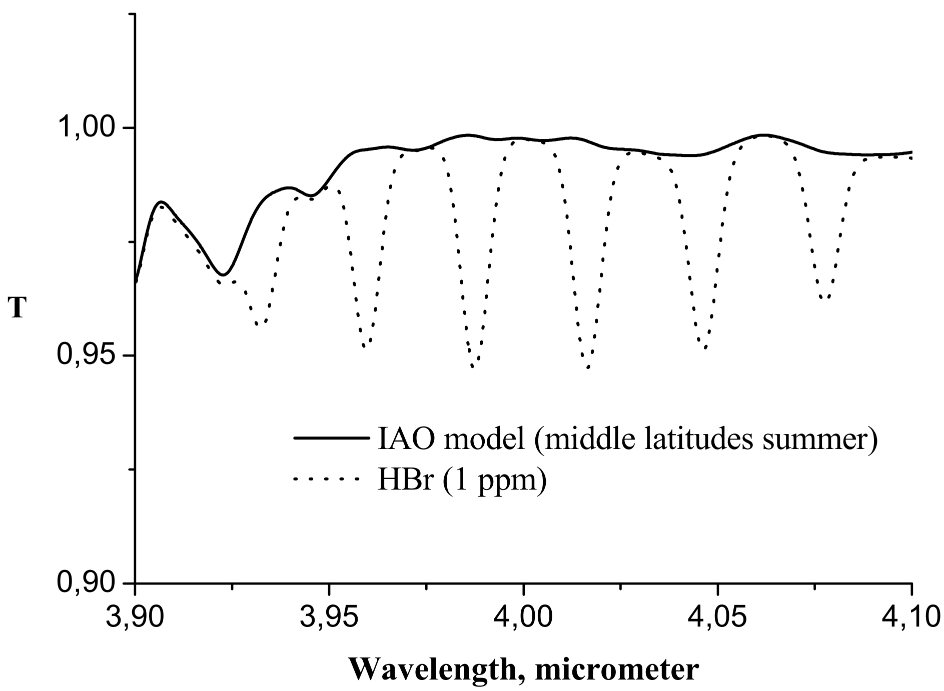

Figure 2. Air transmission spectrum for a path 1 km long (HBr; lasing line width 5 cm^{-1})

Table 3. Wavelengths chosen for HBr sounding in the 3–4 μm region

$\lambda_{ab.}$, μm (in air)	$N_{ab.}$, cm^{-1} (in air)	T_{HBr} 1 cm^{-1}	$T_{int. ab.}$ 1 cm^{-1}	T_{HBr} 5 cm^{-1}	$T_{int. ab.}$ 5 cm^{-1}
On-line 3.95955	2525.539	0.82	0.99	0.95	0.98
Off-line 3.96269	2523.538	0.99	0.99	0.96	0.98
On-line 3.9873	2507.962	0.79	0.99	0.94	0.99
Off-line 3.99005	2506.234	0.99	0.99	0.95	0.99
On-line 4.01634	2489.829	0.79	0.99	0.94	0.98
Off-line 4.01279	2492.031	0.99	0.99	0.96	0.99
On-line 4.04642	2471.320	0.81	0.97	0.95	0.97
Off-line 4.05281	2467.423	0.99	0.98	0.98	0.98
On-line 4.07744	2452.519	0.85	0.97	0.96	0.97
Off-line 4.0718	2455.916	0.99	0.99	0.98	0.98

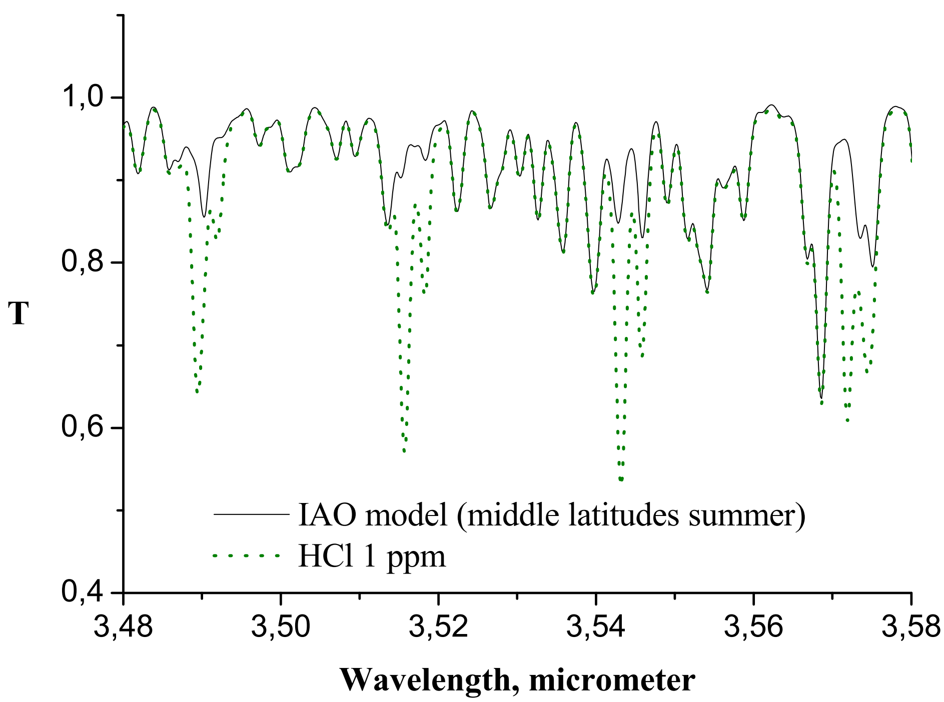

Figure 3. Air transmission spectrum for a path 1 km long (HCl; lasing line width 1 cm^{-1})

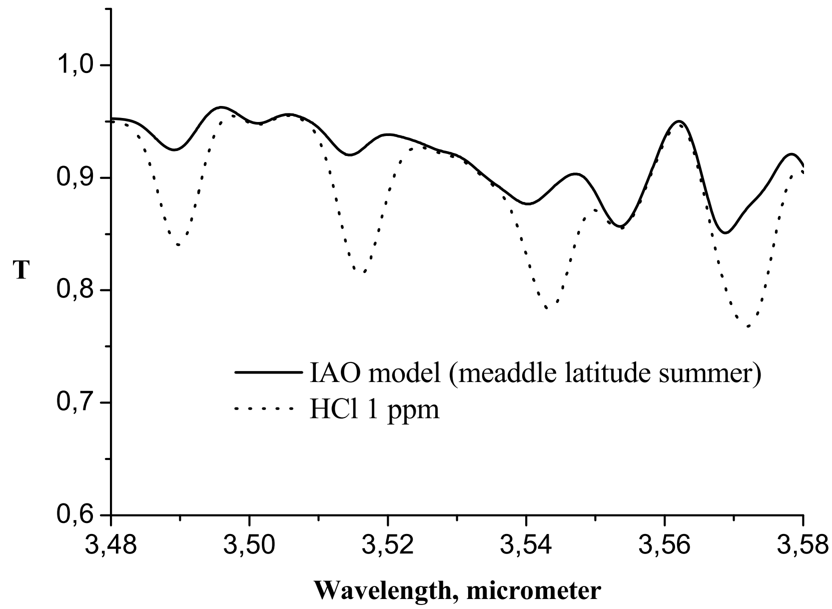

Figure 4. Air transmission spectrum for a path 1 km long (HCl; lasing line width 5 cm^{-1})

Table 4. Wavelengths chosen for HCl sounding in the 3–4 μm region

$\lambda_{ab.}$, μm (in air)	$N_{ab.}$, cm^{-1} (in air)	T_{HCl}	$T_{int. ab.}$	T_{HCl}	$T_{int. ab.}$
		1 cm^{-1}		5 cm^{-1}	
On-line 3.4895	2865.740	0.64	0.89	0.84	0.89
Off-line 3.49548	2860.837	0.98	0.97	0.94	0.94
On-line 3.51576	2844.335	0.57	0.91	0.81	0.92
Off-line 3.51985	2841.030	0.95	0.96	0.88	0.93
On-line 3.54318	2821.829	0.52	0.85	0.78	0.88
Off-line 3.5477	2818.727	0.96	0.96	0.85	0.89
On-line 3.57191	2799.622	0.60	0.93	0.76	0.85
Off-line 3.5769	2795.716	0.97	0.97	0.87	0.90

To estimate capabilities of remote atmospheric gas analysis at the HBr and HCl sounding wavelength chosen in the lasing range of the KTA-based OPO-laser, echo signals were calculated for a vertical path with accounting for interfering absorption of all main atmospheric gas components; the concentration of a gas sounded was assumed equal to 1 ppm. The McClatchey [5] and Zuev and Komarov [6] atmospheric optical-meteorological models were used in the calculations. Spectral parameters of atmospheric gas absorption lines were taken from the HITRAN databank [7] neglecting spectral data errors. The backscattering coefficients used in the calculations were determined using statistical profiles of lidar ratios from the Krekov and Rakhimov model [8].

Input data for the numerical simulation are given in Table 5.

Table 5. Input data for numerical simulation of laser sounding

Lidar system parameter	**Parameter value**
Receiver area $A_{rec.}$(D=0.3 m)	7 10^{-8} km^2
Instrumental function width	1 cm^{-1} (HBr sounding) 1 cm^{-1}, 5 cm^{-1} (HCl sounding)
Receiving system efficiency	0.3
Spatial resolution ΔR	1 km
Pulse energy maximum	5 mJ
Pulse frequency	10 Hz
Pulse length	10–13 ns
Radiation divergence angle	2 mrad
Laser tuning range	3–4 µm
Aerosol backscattering coefficient β_π	2.3$\cdot$ 10^{-3} km^{-1}
Photodetector NEP	$1\cdot10^{-9}$ W

Simulation results are given in Figs. 5–7 and Tables 6–8.

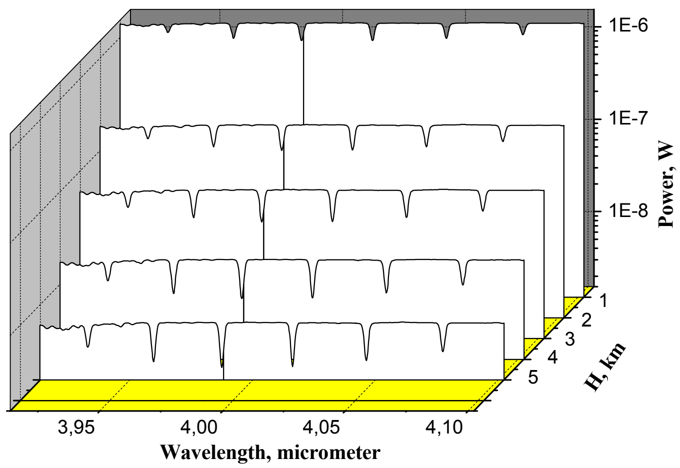

Figure 5. Spatially and spectrally resolved lidar echo signals in the region of HBr sounding wavelengths chosen (instrumental function width 1 cm^{-1})

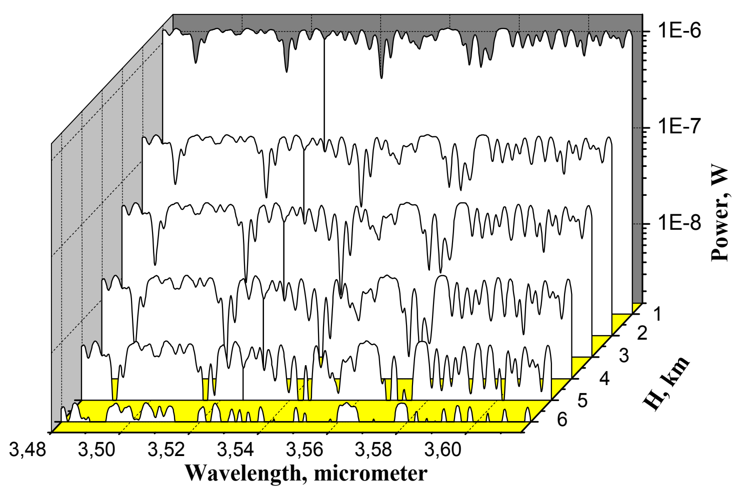

Figure 6. Spatially and spectrally resolved lidar echo signals in the region of HCl sounding wavelengths chosen (instrumental function width 1 cm^{-1})

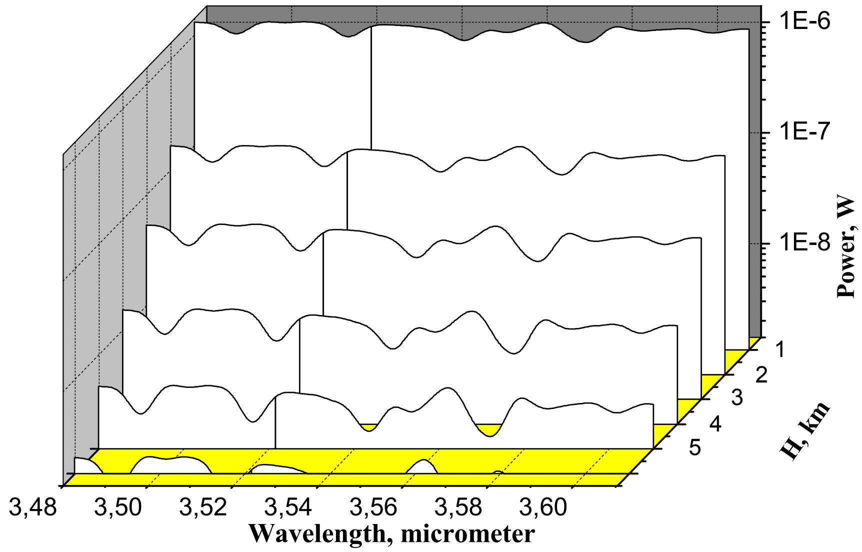

Figure 7. Spatially and spectrally resolved lidar echo signals in the region of HCl sounding wavelengths chosen (instrumental function width 5 cm^{-1})

Table 6. Lidar echo signals for HBr sounding wavelengths chosen (instrumental function width 1 cm^{-1})

Gas	Wavelength, μm	Lidar signal power, W				
		1 km	2 km	3 km	4 km	5 km
HBr	3.96269 “off line”	$1.40\ 10^{-6}$	$1.85\ 10^{-7}$	6.1610^{-8}	$1.80\ 10^{-8}$	$6.29\ 10^{-9}$
	3.95955 “on line”	$9.68\ 10^{-7}$	$1.08\ 10^{-7}$	$3.09\ 10^{-8}$	$7.87\ 10^{-9}$	$2.41\ 10^{-9}$
	3.99005 “off line”	$1.40\ 10^{-6}$	$1.85\ 10^{-7}$	$6.15\ 10^{-8}$	$1.79\ 10^{-8}$	$6.28\ 10^{-9}$
	3.9873 “on line”	$9.13\ 10^{-7}$	$9.98\ 10^{-8}$	$2.78\ 10^{-8}$	$6.94\ 10^{-9}$	$2.09\ 10^{-9}$
	4.01279 “off line”	$1.40\ 10^{-6}$	$1.87\ 10^{-7}$	$6.22\ 10^{-8}$	$1.82\ 10^{-8}$	$6.37\ 10^{-9}$
	4.01634 “on line”	$9.15\ 10^{-7}$	$1.00\ 10^{-7}$	$2.81\ 10^{-8}$	$7.04\ 10^{-9}$	$2.13\ 10^{-9}$
	4.05281 “off line”	$1.40\ 10^{-6}$	$1.86\ 10^{-7}$	$6.20\ 10^{-8}$	$1.81\ 10^{-8}$	$6.30\ 10^{-9}$
	4.04642 “on line”	$9.67\ 10^{-7}$	$1.09\ 10^{-7}$	$3.12\ 10^{-8}$	$8.03\ 10^{-9}$	$2.49\ 10^{-9}$
	4.0718 “off line”	$1.40\ 10^{-6}$	$1.87\ 10^{-7}$	$6.21\ 10^{-8}$	$1.82\ 10^{-8}$	$6.36\ 10^{-9}$
	4.07744 “on line”	$1.05\ 10^{-7}$	$1.23\ 10^{-7}$	$3.66\ 10^{-8}$	$9.72\ 10^{-9}$	$3.11\ 10^{-9}$

Table 7. Lidar echo signals for HCl sounding wavelengths chosen (instrumental function width 1 cm^{-1})

Gas	Wavelength, μm	Lidar signal power, W				
		1 km	2 km	3 km	4 km	5 km
HCl	3.49548 “off line”	$1.37\ 10^{-6}$	$1.81\ 10^{-7}$	5.9810^{-8}	$1.74\ 10^{-8}$	$6.04\ 10^{-9}$
	3.4895 “on line”	$6.05\ 10^{-7}$	$5.58\ 10^{-8}$	$1.34\ 10^{-8}$	$2.93\ 10^{-9}$	–
	3.51985 “off line”	$1.30\ 10^{-6}$	$1.67\ 10^{-7}$	$5.39\ 10^{-8}$	$1.54\ 10^{-8}$	$5.26\ 10^{-9}$
	3.51576 “on line”	$4.86\ 10^{-7}$	$4.08\ 10^{-8}$	$8.98\ 10^{-9}$	$1.81\ 10^{-9}$	–
	3.5477 “off line”	$1.32\ 10^{-6}$	$1.70\ 10^{-7}$	$5.56\ 10^{-8}$	$1.60\ 10^{-8}$	$5.51\ 10^{-9}$
	3.54318 “on line”	$4.17\ 10^{-7}$	$3.24\ 10^{-8}$	$6.64\ 10^{-8}$	$1.25\ 10^{-9}$	–
	3.5769 “off line”	$1.34\ 10^{-6}$	$1.75\ 10^{-7}$	$5.73\ 10^{-8}$	$1.65\ 10^{-8}$	$5.72\ 10^{-9}$
	3.57191 “on line”	$5.48\ 10^{-7}$	$4.83\ 10^{-8}$	$1.11\ 10^{-8}$	$2.34\ 10^{-9}$	–

Table 8. Lidar echo signals for HCl sounding wavelengths chosen (instrumental function width 5 cm^{-1})

Gas	Wavelength, μm	Lidar signal power, W				
		1 km	2 km	3 km	4 km	5 km
HCl	3.49548 “off line”	$1.27\ 10^{-6}$	$1.62\ 10^{-7}$	5.1910^{-8}	$1.47\ 10^{-8}$	$5.00\ 10^{-9}$
	3.4895 “on line”	$1.02\ 10^{-6}$	$1.18\ 10^{-7}$	$3.48\ 10^{-8}$	$9.16\ 10^{-9}$	2.9110^{-9}
	3.51985 “off line”	$1.11\ 10^{-6}$	$1.33\ 10^{-7}$	$4.04\ 10^{-8}$	$1.09\ 10^{-8}$	$3.54\ 10^{-9}$
	3.51576 “on line”	$9.58\ 10^{-7}$	$1.07\ 10^{-7}$	$3.09\ 10^{-8}$	$7.93\ 10^{-9}$	$2.46\ 10^{-9}$
	3.5477 “off line”	$1.04\ 10^{-6}$	$1.22\ 10^{-7}$	$3.62\ 10^{-8}$	$9.59\ 10^{-8}$	$3.05\ 10^{-9}$
	3.54318 “on line”	$8.88\ 10^{-7}$	$9.65\ 10^{-8}$	$2.68\ 10^{-8}$	$6.69\ 10^{-9}$	$2.02\ 10^{-9}$
	3.5769 “off line”	$1.09\ 10^{-6}$	$1.30\ 10^{-7}$	$3.91\ 10^{-8}$	$1.04\ 10^{-8}$	$3.38\ 10^{-9}$
	3.57191 “on line”	$8.53\ 10^{-7}$	$9.10\ 10^{-8}$	$2.48\ 10^{-8}$	$6.09\ 10^{-9}$	$1.81\ 10^{-9}$

The above results show that the level of lidar echo signals for all gases exceeds the level of noise equivalent power of the photodetector NEP = 10^{-9} W throughout the 0–5 km altitude range considered.

4. CONCLUSIONS

The numerical simulation carried out shows that a KTA-crystal based OPO-laser is a promising radiation source for remote sounding of trace atmospheric gases along surface tropospheric paths. The laser system design provides for a possibility of narrowing a lasing line in the 0.01–5 cm^{-1} limits. Possibilities of such improvement, along with a small step of laser radiation wavelength tuning and the presence of absorption lines of other atmospheric gases, in particular, air pollutants, in the spectral range under study make this laser source a unique instrument for designing a ground-based differential absorption lidar.

ACKNOWLEDGMENTS

This work was supported by the Ministry of Science and Education of the Russian Federation (Agreement No. 14.604.21.0046 - Unique identifier RFMEFI60414X0046).

REFERENCES

[1] Fiorani L., S. Babichenko, J. Bennes, R. Borelli, R. Chirico, A. Dolfi-Bouteyre, L., L. Hespel, T. Huet, V. Mitev, A. Palucci, M. Pistilli, A. Puiu, O. Rebane, "Lidar detection of explosive percursors", 26th ILRC, 25-29 June 2012, Portohelli – Greece, Proceedings Vol. I, 231-234 (2012).

[2] V. Mitev, S. Babichenko, J. Bennes, R. Borelli, A. Dolfi-Bouteyre, L. Fiorani, L. Hespel, T. Huet, A. Palucci, M. Pistilli, A. Puiu, O. Rebane, I. Sobolev, "Mid-IR DIAL for high-resolution mapping of explosive precursors", Lidar Technologies, Techniques, and Measurements for Atmospheric Remote Sensing IX, edited by Upendra N. Singh, Gelsomina Pappalardo, Proc. of SPIE Vol. 8894, 88940S (2013).

[3] Geiko, P.P., Privalov, V.E., Romanovskii, O.A. , Kharchenko, O.V.Application of frequency converters to femtosecond laser radiation for lidar monitoring of the atmosphere, "Optics and Spectroscopy", 108 (1), 80-85 (2010).

[4] Romanovskii, O.A., Kharchenko, O.V., Yakovlev, S.V. Methodological aspects of lidar ranging of trace gases in the atmosphere by differential absorption, "Journal of Applied Spectroscopy" 79 (5), 793-800 (2012).

[5] McClatchey, R. A., Fenn, R.,W., Selby, J. E. A., Volz, F. E. and Garing, J. S., [Optical properties of atmosphere], *Report AFCRL-71-0297*, Bedford, Mass (1971).

[6] Zuev, V.E., Komarov, V.S. [Statistical Models of the Temperature and Gaseous Components of the Atmosphere] [in Russian], Leningrad: Gidrometeoizdat (1986).

[7] Rothman, L. S., Gordon, I. E., Barbe, A., Chris Benner, D., Bernath, P. F., Birk, M., Boudon, V., Brown, L. R., Campargue, A., Champion, J.-P., Chance, K., Coudert, L. H., Dana, V., Devi, V. M., Fally, S., Flaud, J.-M., Gamache, R. R., Goldman, A., Jacquemart, D., Kleiner, I., Lacome, N., Lafferty, W. J., Mandin, J.-Y., Massie, S. T., Mikhailenko, S. N., Miller, C. E., Moazzen-Ahmadi, N., Naumenko, O. V., Nikitin, A. V., Orphal, J., Predoi-Cross, A., Perevalov, V. I., Perrin, A., Rinsland, C. P., Rotger, M., Simeckov, M., Smith, M. A. H., Sung, K., Tashkun, S., Tennyson, J., Toth, R. A.,. Vandaele, A. C. and Vander Auwera J., "The HITRAN 2008 molecular spectroscopic database," Journal of Quantitative Spectroscopy and Radiative Transfer 110 (9-10), 533-572 (2009).

[8] Krekov, G. M. and Rakhimov, R. F., [Optical Location Model of Continental Aerosol] [In Russian], Novosibirsk: Nauka (1982).